

## **Supplementary Information**

### **SI Materials and Methods**

#### **Cell Culture**

Human hepatocellular carcinoma cell lines were obtained from the American Type Culture Collection (ATCC; [www.atcc.org](http://www.atcc.org)) and were cultured according to standard mammalian tissue culture protocols and sterile technique. SNU398 (ATCC no. CRL-2233) and SNU475 (ATCC no. CRL-2236) cells were maintained in Roswell Park Memorial Institute (RPMI) 1640 Medium, and HepG2 (ATCC no. HB-8065) cells were maintained in Dulbecco's Modified Eagle Medium (DMEM). All media (from GIBCO) were supplemented with 10% fetal bovine serum (Sigma-Aldrich) and 1% penicillin/streptomycin (GIBCO). Venor™ GeM Mycoplasma Detection Kit (Sigma-Aldrich) was used every month to confirm all cell lines were mycoplasma-free.

#### **Drug treatment and cell doubling time measurement**

$3 \times 10^5$  SNU398, SNU475 and HepG2 cells were untreated or treated with three daily consecutive doses of SGI-110 (Astex Pharmaceuticals, Dublin, CA), or 5-aza-CdR (Sigma-Aldrich) at 100 nM (72 h exposure) before drug removal or GSK126 (#A-1275, Active Biochem, LTD, Hong Kong) at 500 nM daily. At subsequent time points indicated at Figure 2A, cells were harvested, re-suspended, and counted using a Coulter counter analyzer (Beckman Coulter, Inc.), and  $3 \times 10^5$  cells were reseeded into fresh 100 mm culture dishes. Doubling

time (in days) was calculated as follows: Doubling time =  $A \cdot \text{LOG}(2) / (\text{LOG}(B) - \text{LOG}(C))$ , where A is the number of days since the cells were plated, B is the total number of cells when the cells were harvested, and C is the number of cells seeded.

### **Apoptosis and Cell Cycle Analysis**

SNU398 cells ( $3 \times 10^5$ ) were untreated or treated with three daily consecutive doses of SGI-110 at 100 nM, and cells were harvested at day 10 after drug treatment. Cellular apoptosis was measured by annexin V and propidium iodide (PI) staining using annexin V-FITC apoptosis detection kit (MBL) according to the manufacturer's protocol. After staining the cells were analyzed by MoFlo Astrios Cell Sorter (Beckman Coulter, Inc.). Annexin V-FITC staining indicated apoptotic cells.

For cell cycle analysis, cells were fixed with 66% ethanol and stored at 4°C until ready to stain with propidium iodide (PI). Fixed cells were pelleted and resuspended in 500  $\mu$ l of PI staining solution (PBS + 100  $\mu$ g/ml RNase A + 50  $\mu$ g/ml PI) and incubated overnight at 4°C. For flow cytometry analysis, cells were filtered through cell strainer snap caps (Fisher Scientific) and then analyzed on a CytoFLEX S (Beckman Coulter). Cell cycle data were analyzed using ModFit LT software (Verify Software House, [www.vsh.com](http://www.vsh.com)) and apoptosis was measured using FlowJo v10.0.7 (FlowJo, LLC).

### ***M.SssI* Treatment**

*M.SssI* treatment was performed as previously described(1, 2). Briefly,  $5 \times 10^5$  cells were harvested, washed with cold PBS, cell pellets were collected and lysed in 1 ml of Lysis Buffer (10 mM Tris pH 7.4, 10 mM NaCl, 3 mM MgCl<sub>2</sub>, 0.1 mM EDTA, 0.5% NP-40), followed by centrifugation at 500 x g for 10 min at 4°C. The nuclei were collected and washed in 2 ml Wash Buffer (10 mM Tris pH 7.4, 10 mM NaCl, 3 mM MgCl<sub>2</sub>, 0.1 mM EDTA), then separated into two microcentrifuge tubes (no enzyme control and *M.SssI* reaction, respectively), and centrifuged at 500 x g for 10 min at 4°C. The nuclei were resuspended in 150 µl reaction mix containing 76 µl ddH<sub>2</sub>O, 15 µl 10X NEBuffer 2, 45 µl 1 M sucrose, 1.5 µl 32 mM S-adenosylmethionine (SAM), and 12.5 µl 4 U/µl *M.SssI* (or ddH<sub>2</sub>O for no enzyme control). The reaction mixtures were flicked to mix, then incubated at 37°C for 15 minutes. Pre-warmed (37°C) 300 µl Stop Solution (10 mM Tris-HCl pH 7.9, 600 mM NaCl, 1% SDS, 0.1 mM EDTA) and 6 µl Proteinase K (Roche) were added to each tube, and each reaction mixture was incubated at 55°C overnight. The DNA was then purified by phenol/chloroform extraction and ethanol precipitation, then re-dissolved in 50 µl 1X TE pH 8.0 for subsequent analyses.

### **Quality Control for *M.SssI* Treatment**

*M.SssI*-treated DNA or no enzyme control DNA (1 ug each) underwent bisulfite conversion using the Zymo EZ DNA Methylation Kit (Zymo research). Bisulfite (BS)-converted DNA was analyzed via high resolution melt (HRM) analysis using

the Bio-Rad Precision Melt Supermix (Bio-Rad) in 20 µl reactions containing 10 µl Precision Melt Supermix, 1 µl primer mix (5 µM for each primer), 1 µl BS-converted DNA, 8 µl ddH<sub>2</sub>O). The protocol for PCR was: 95°C for 2 min, [95°C for 10 s, 58°C for 30 s, plate read, 72°C for 30 s] x 60 cycles, 95°C for 30 s, 60°C for 1 min, Melt Curve 65°C to 90°C [10 s and plate read at each degree]. Primer sequences were listed in Supplementary Table 1. Proper M.SssI treatment was verified via a shift in melting curves upon methylation. DNA samples with verified M.SssI treatment (0.5 ug) were then submitted for HM450 analysis.

### **Infinium® HumanMethylation450 BeadChip Assay**

The amount of bisulfite-converted DNA and the completeness of bisulfite conversion were determined using a panel of MethyLight-based quality control (QC) tests as described previously (3). All samples passed these QC tests and entered the HM450 assay data production pipeline (4). The subsequent HM450 assay was performed at the University of Southern California Molecular Genomics Core Facility according to the manufacturer's specifications (Illumina). Each sample was processed using the Infinium DNA methylation assay data production pipeline as described in (5). After the chemistry steps, BeadArrays were scanned and the raw signal intensities were extracted from the \*.IDAT files using the R package *methyumi*. The intensities were corrected for background fluorescence and red-green dye-bias (6). The beta-values were calculated as  $(M/(M+U))$ , in which M and U refer to the (pre-processed) mean methylated and unmethylated probe signal intensities, respectively. The HM450 probes,

interrogating 482,421 CpG sites, were filtered to remove probes with fluorescent intensity statistically insignificant above background signal (detection p-value >0.05), located within 15 base pairs of a single nucleotide polymorphism, mapped to multiple locations, or on the sex chromosomes. The end result is a dataset of corrected beta-values for 385,826 probes which cover ~19,500 genes.

### **AcceSss/ble Assay Data Analysis**

AcceSss/ble assay data analysis has been described in our previous publications (1, 2). Corrected  $\beta$ -values (range 0-1) of no enzyme control (NoE, endogenous methylation values for each CpG locus) were then subtracted from corrected  $\beta$ -values of M.SssI-treated samples to obtain DNA accessibility values (Acc) for each CpG site. Acc and NoE values for each sample after SGI-110 treatment at a given time point (D3 up to D31) were then subtracted from the respective values in the untreated samples (D0), resulting in delta-methylation ( $\Delta$ Meth) and delta-accessibility ( $\Delta$ Acc) values.  $\Delta$ Meth and  $\Delta$ Acc values ( $\Delta\beta$ -values) were used in subsequent analyses as values for changes in DNA methylation and accessibility, using a cutoff of  $\Delta\beta$ -value  $\pm 0.3$  for changes at each locus (2). Six groups with different methylation and chromatin accessibility changes were identified as groups a-f in Figure 3 and S4.

### **Gene Expression Analysis**

Total RNA was extracted with Trizol reagent (Invitrogen), followed by clean-up and DNase I treatment with Zymo Direct-Zol RNA mini prep kit (Zymo Research)

according to the manufacturer's protocol. RNA quality was assessed using Agilent 2100 bioanalyzer with RNA Nano chips (Agilent Technologies, Inc.). Expression analysis was performed at Sanford-Burnham Medical Institution (La Jolla, CA) using the Illumina genome-wide expression BeadChip (HumanHT-12\_V4.0\_R1) (Illumina). Gene expression data were processed using the *lumi* package in R. The data were  $\log_2$ -transformed and normalized using quantile normalization as previously described (4).

### **Integration with TCGA DNA Methylation and RNA-seq data**

TCGA LIHC HM450 DNA methylation and RNA sequencing (RNA-seq) data were downloaded from TCGA Data Portal (<https://tcga-data.nci.nih.gov/tcga/>). Unsupervised hierarchical clustering and Multidimensional Scaling (MDS) were performed based on the top 1% most variably methylated probes among the HM450 data for TCGA tumors, adjacent-normal tissues, as well as untreated SNU398, HepG2, and SNU475 cells, using the *hclust* and *cmdscale* functions in R, respectively.

For integration with TCGA RNA-seq data, we first identified the most frequently altered genes in 41 pairs of primary HCC tumors compared to their adjacent normal tissues using a 4-fold expression cut-off. We next identified SGI-110 target genes that were frequently altered in these primary HCC tumors by intersecting with the expression profiles of the three HCC cells before and after SGI-110 treatment. To examine DNA methylation and chromatin accessibility

status for these genes, we filtered the illumina HM450 probes for those that are located within 200 bp upstream of transcription start sites (TSS200) as “promoter” probes, and those “gene body” probes according to illumina’s annotations. To examine EZH2 and H3K27me3 occupancy levels at gene promoters, the processed EZH2 and H3K27me3 Chip-seq data for HepG2 cells were obtained from the ENCyclopedia of DNA Elements (ENCODE) public data portal (<http://genome.ucsc.edu/ENCODE/>). HM450 probes and the Chip-seq peaks were intersected using BedTools (<http://bedtools.readthedocs.org/en/latest/index.html>).

### **Pathway Analysis**

GO and pathway enrichment analysis and functional annotation clustering were performed using the Database for Annotation, Visualization and Integrated Discovery (DAVID) database v6.8. Relevant GO lists were ranked according to their p value as determined by DAVID.

### **Survival Analyses**

For the log-rank (Mantel-Cox) survival analyses in Figure 5E, we utilized the available follow-up survival data on 192 patients from the TCGA HCC dataset (7). We screened top 50 SGI-110 target genes that were frequently up- or down-regulated in TCGA HCC patients, and HCC samples were stratified by high and low expression quartiles of these genes. HCC patients in the lowest quartile of expression were compared for overall survival to those in the highest quartile of

gene expression by log-rank survival analysis. Among these genes, *NFYA*, *NFYB* and *NFYC* expression levels were found to correlate with patient survival. GraphPad Prism (v6. 03) software was used to analyze and plot the data.

### **Quantitative Real-Time RT-PCR**

The expression of ERVs and a panel of SGI-110 target genes were measured by real-time quantitative reverse transcription polymerase chain reaction (qRT-PCR) using KAPA SYBR FAST universal 2× qPCR master mix (KAPA) with primers listed in the Supplementary Table 1. TATA-Box Binding Protein (*TBP*) and Glyceraldehyde 3-phosphate dehydrogenase (*GAPDH*) were used as reference genes.

### **Western Blot Analysis**

HepG2, SNU398 and SNU475 cells ( $3 \times 10^5$ ) were untreated or treated with 300 nM 5-aza-CR, 100 nM 5-aza-CdR, or 100 nM SGI-110 for 72 h. Cells were then trypsinized, washed with PBS and resuspended in RIPA buffer (50 mM Tris-HCl, pH 8.0, 150 mM NaCl, 1% NP-40, 0.5% sodium deoxycholate and 0.1% SDS) with protease inhibitors. The cells were then sonicated on ice and cellular debris was removed by centrifugation. Protein (30 µg) was mixed with SDS/β-mercaptoethanol loading buffer and resolved on a Biorad 4-15% gradient SDS/PAGE gel. Antibodies against the DNMT1 (Abcam, ab134148), DNMT3A (Cell Signaling, #2160), DNMT3B (Novus Biologicals, NB100-56514), and p53



(Santa Cruz Biotechnology, sc-126) were used. Proteins were visualized using the ECL detection system (Thermo Scientific) and ChemiDoc™ system (BioRad).

### **Statistical analysis**

Statistical tests were conducted using R software (R version 3.1.2, R Development Core Team, <https://cran.r-project.org/>). The R package “plogcor” was used to calculate a matrix consisting of p-values and Pearson correlations between gene expression and DNA methylation, as well as between gene expression and chromatin accessibility. Wilcoxon rank-sum test was used to assess statistical significance for expression differences of between normal and primary HCC tumor samples in TCGA RNA-seq dataset for UHRF1, EZH2, EED and SUZ12 genes. P-values less than 0.05 were considered significant.

### **Accession codes and reviewer access links**

All data have been deposited at the Gene Expression Omnibus (GEO) (<http://www.ncbi.nlm.nih.gov/geo/>) with accession code GSE105067 (<https://www.ncbi.nlm.nih.gov/geo/query/acc.cgi?acc=GSE105067>).

## SI References

1. Becket E, *et al.* (2016) Identification of DNA Methylation-Independent Epigenetic Events Underlying Clear Cell Renal Cell Carcinoma. *Cancer Res* 76(7):1954-1964.
2. Pandiyan K, *et al.* (2013) Functional DNA demethylation is accompanied by chromatin accessibility. *Nucleic Acids Res* 41(7):3973-3985.
3. Campan M, Weisenberger DJ, Trinh B, & Laird PW (2009) MethyLight. *Methods Mol Biol* 507:325-337.
4. Yang X, *et al.* (2014) Gene body methylation can alter gene expression and is a therapeutic target in cancer. *Cancer Cell* 26(4):577-590.
5. Bibikova M, *et al.* (2011) High density DNA methylation array with single CpG site resolution. *Genomics* 98(4):288-295.
6. Triche TJ, Jr., Weisenberger DJ, Van Den Berg D, Laird PW, & Siegmund KD (2013) Low-level processing of Illumina Infinium DNA Methylation BeadArrays. *Nucleic Acids Res* 41(7):e90.
7. Cancer Genome Atlas Research Network. Electronic address wbe & Cancer Genome Atlas Research N (2017) Comprehensive and Integrative Genomic Characterization of Hepatocellular Carcinoma. *Cell* 169(7):1327-1341 e1323.

**Supplementary Table 1: Primers used in this study.**

<b>qPCR primers</b>	<b>Forward</b>	<b>Reverse</b>
<b>A. Primers for ERVs</b>		
1 HERV-W	TGAGTCAATTCTCATACCTG	AGTTAAGAGTTCTTGGGTGG
2 HML-2	AAAGAACCAGCCACCAGG	CAGTCTGAAAACCTTTTCTCTC
3 HML-3	CTGCAGCCTGCTAAGCG	CACTGTGAAAATTTTTTACGAG
4 HML-5	CAAGCTTTGCTCCCCAGTAG	TTGGGGCTGCTGGTAAAATA
5 HERV-L	TTCGTTGGTTTAGGGGTTTC	TCAGCATTTTTGGGTCTAATCA
7 HERV-I	ATGCCTGCTTCAATATGTCG	TGAGGCAAGGGTAAGGACAC
8 HERV-IP-T47D	GGGCGGAAACAACAATATCA	GGGGAGTCTGTGAACCCTTG
10 HERV-H	CACAGACAGCCCCATTACT	GGGAGAGCACGTGTGTTTTT
11 Seq61	TTCACATGGACTGACCCTGA	GTAATGGGGGCTGTCTCTGA
12 RGH2	CGCCACACTTCAATCTCTCC	CGTGGTCTGACACCTCTGAA
13 Harlequin	GAGGTCCAGCCCTGATACTG	CGATCACATTCAATGCTTGC
14 MER21C	CCCTCCACAGGGTAACAATG	AGCTGGAGAAAGCATGGAAA
15 HML-1	TGCTTTTACTGTTCCCTGCCATA	GCTATTTAACATGCCCTGTGG
17 Seq39	TTTTTCTCCATTCTGTCCA	TATTTCTGGCCTTGCCAACT
18 Seq40	AGCAATTTGCCTTCAGTTGG	TGGCACACAAATATCTCACCA
19 Seq45	TATAAGGCCACCAGAAGCA	CTGGCATGCAAACATCTCAC
20 Seq48	TGATCACTTTTTGCTTCCACA	CTTGCTCTTTTGATCCGTCAG
21 Seq51	CACTGGCAAGGTCAGCAATA	CACGCAAATGTCTCACCAAT
26 HW33438	ATGACCCGCAGCTTCTAACAG	CTCCGCTCACAGAGCTCCTA
27 HW38223	TGAGCTTTCCCTCACTGTCC	TGTTCCGGCTTGATTAGGATG
28 envW	CCCCATCGTATAGGAGTCTT	CCCCATCAGACATACCAGTT
29 spervwe1	CGGACATCCAAAGTGATACATCCT	GGTTCCTTAGAAAGACTCC
MLT1N2	AATTGTGTGGGTTGGCAAGT	GAATCTCTCTGAAGAAGCAGCA
LTR12C	CTCTTAAGGTGGCGCATCTG	AAGGTCTGCAGCTTCACTCC
HERV-Fc1	TTCCCACCGCTGGTAATAG	AGGCTAAGGATTCCGGCTGAG
HW-family-1	AAGAATCCCTAAGCCTAGCTGG	GCCTAATTAGCATTTTAGTGAGCTC
HW-family-2	CAACATTCCATTCTTGGGAATC	TTCCAAGATGGTGGCAAGC
ERVK	AGAGGAAGGAATGCCTCTTGCGAG	TTACAAAGCAGTATTGCTGCCCGC
ERV3-int	GAGACCAGCAGACGGTAAGG	CCAAGGCCACAGATGGTACT
<b>B. Primers for SGI-110 target genes</b>		
MT1F	CCACTGCTTCTTCGCTTCTC	GCATTTGCACTCTTTGCACT
MT1M	GTCGCTCCATTTATCGCTTG	CTTCTTGCAAGGAGGTGCATT
MT2A	CAACCTGTCCCGACTCTAGC	AGGAGCAGCAGCTTTTCTTG
ALPL	GGCTGTAAGGACATCGCCTA	CCTGGCTTTTCTCGTCACTCT
SEMA3E	ACCCACGATCTTTACAAGC	GGTCCCAGCATCTGATTTGT
NR4A2	AGTCTGATCAGTGCCCTCGT	GCTGGGTGTCATCTCCACTC
PGLYRP2	TGGATCCTACTCGGATTGCT	ACGCAGAAGCTGTGTGTCTG

BHMT	CTGTCTGGACACCACGAAGA	ACCCTCCATCTCCAATCACA
ACSL1	AGTGAGCCTGTTGCTCAGGT	CTGCACAGTTCCTCAAACGA
CAND2	TCCACATCTCCAGCCTCCT	GGATGGAGTCCTTCTGCAAC
CETP	CAGATATCACGGGCGAGAA	ATCAATGGACTTGGCTTCCA
IGFBP1	CTGCGTGCAGGAGTCTGA	CCCAAAGGATGGAATGATCC
RND3	GGCCAGTTTTGAAATCGACA	TCAAAGCAAATCAGCACAGC
FOS	CCGGGGATAGCCTCTCTTAC	GTGGGAATGAAGTTGGCACT
SFRP1	CTACTGGCCCGAGATGCTTA	GTTGTACAGGGAGGACACA
TBP	GCCCGAAACGCCGAATAT	CCGTGGTTCGTGGCTCTCT

### C. Primers for HRM analysis

ACTB	AGAGGGGGTAAAAAATGTTGTAT	TCGAACCATAAAAAACAACCTTTC
GADPH	TTTTAAGATTTTGGGTTGGGT	CTATCGAACAAAAAAACAAAAAAC
C1D	TTTTTGGAGAAGAGTTAAGGAGTAGG	ACTCCAATCTCCCGAAAAAC
RPLP0	AGGTGGTAGTAGTTTAGAGTAAGTTTT	CGAATACAAACAACCATTAAATA

## SI Figures

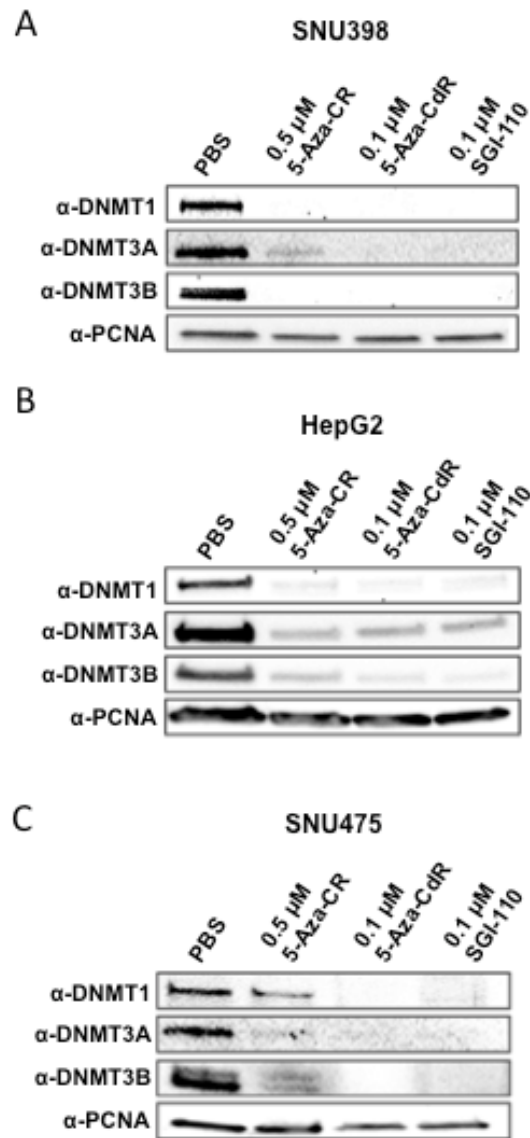


**Figure S1.** Western blot analysis of DNMT1, DNMT3A and DNMT3B levels in HCC cells treated with vehicle control (PBS), 5-Aza-CR, 5-Aza-CdR, and SGI-110. Treatment schedule were shown in Figure 2A and cells were harvested at day 3 after the treatment. PCNA was used as a loading control.

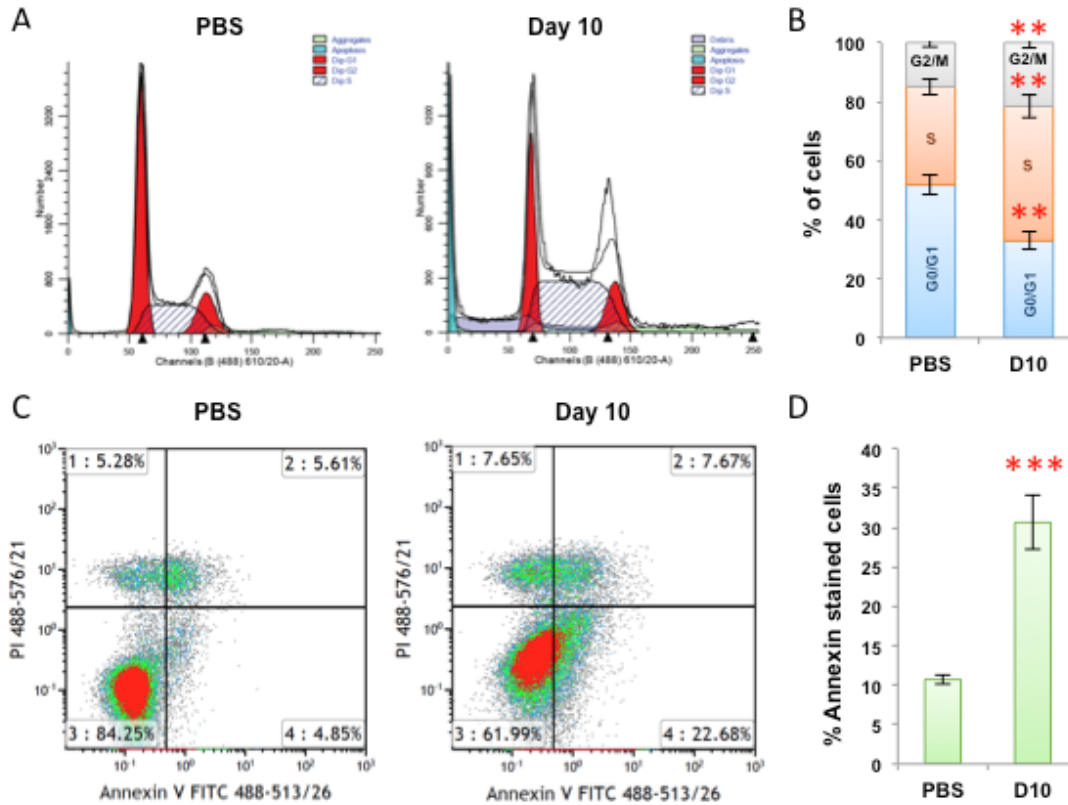


**Figure S2.** SGI-110 treatment induces both cell cycle arrest and apoptosis in SNU398 cells. (A) and (B) Cell cycle analysis of SNU398 cells untreated (PBS) or treated with three daily consecutive doses of SGI-110 at 100 nM. Cells were harvested at day 10 after the treatment and stained with Propidium iodide (PI). Representative PI histogram plots are shown in (A) and bar graph shows quantification of each cell cycle phase (B). Values are presented as mean  $\pm$  SD of three independent experiments. \*\* $p < 0.01$  by Student's t test. (C) and (D) Apoptosis analysis using annexin V-FITC and PI showing an increased percentage of apoptotic cells after SGI-110 treatment. Values are presented as mean  $\pm$  SD of three independent experiments. \*\*\* $p < 0.001$  by Student's t test.

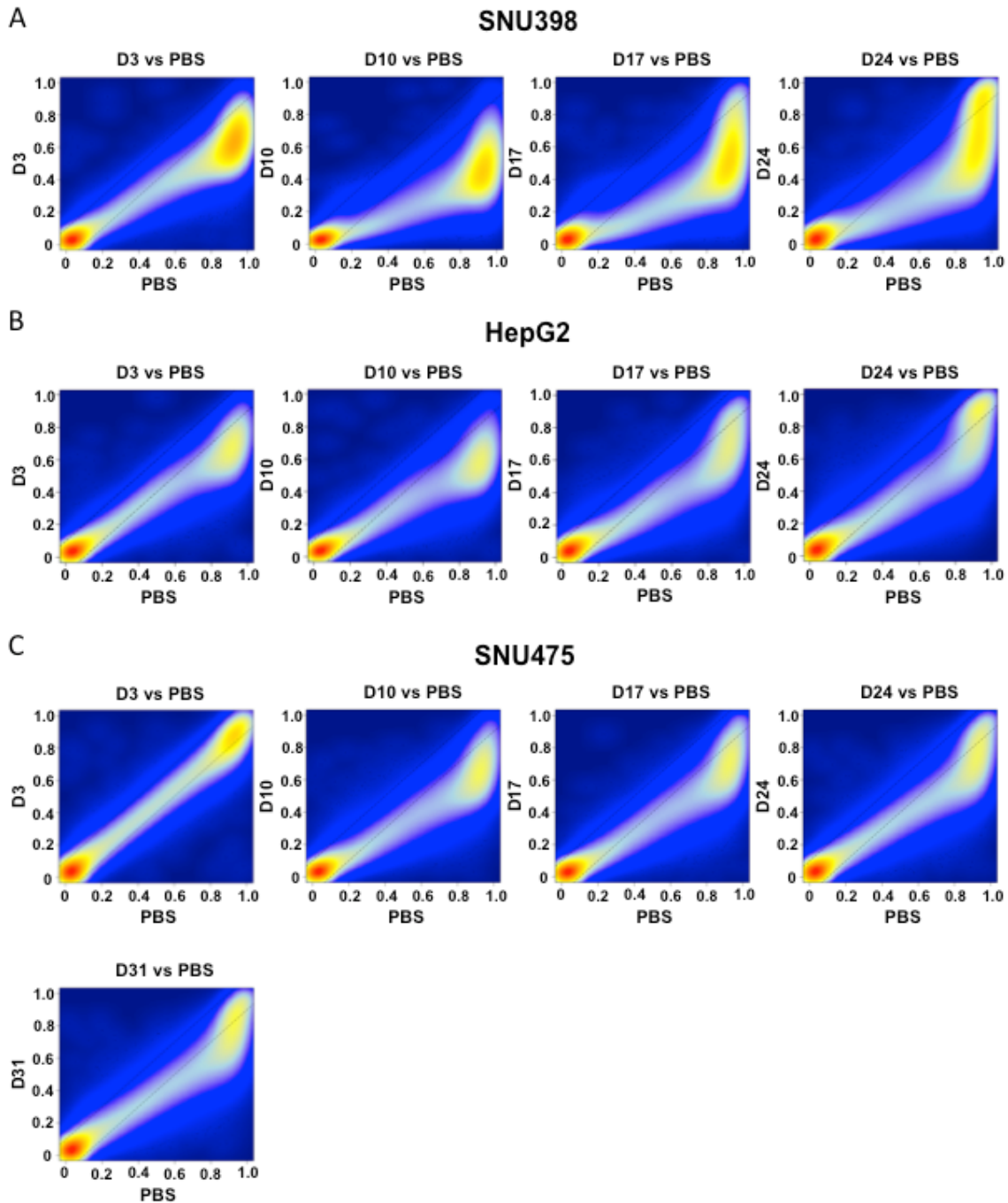


**Figure S3.** Kernel density scatter plots show changes in global DNA methylation patterns after SGI-110 treatment compared to untreated cells at the indicated time points for SNU398, HepG2 and SNU475 cells. The x-axis indicates methylation beta values for vehicle treated control and y-axis indicates beta values for SGI-110 treated HCC cells at each time point after the treatment.

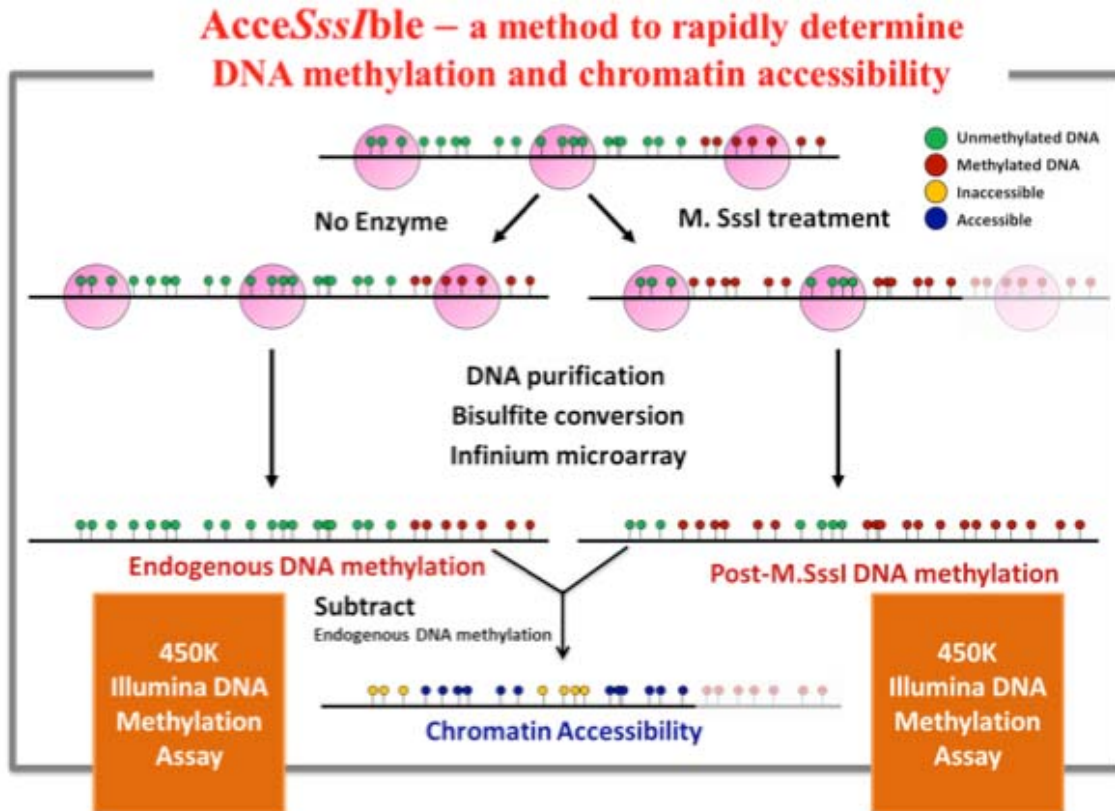


**Figure S4.** Diagram shows the experimental principle and procedures for AcceSss/ble assay (see Method section for details).



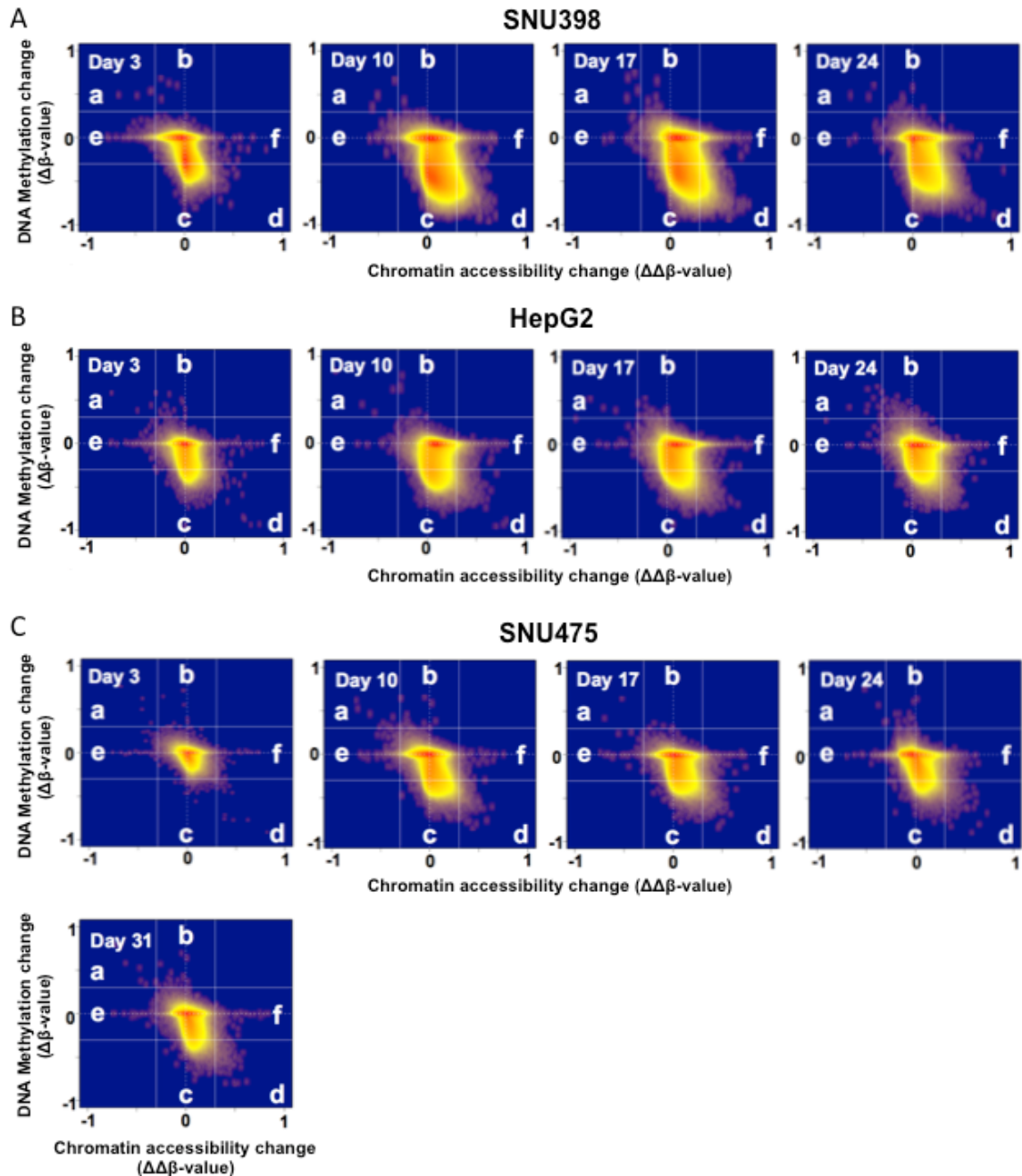


**Figure S5.** Kernel density scatter plot show changes in DNA methylation (as  $\Delta\beta$ -value) versus changes in nucleosome accessibility (as  $\Delta\Delta\beta$ -value) for all 450k probes post SGI-110 treatment during a time course in SNU398, HepG2 and SNU475 cells. A threshold of 0.3 is used for determining both DNA methylation and nucleosome accessibility changes. Six groups of epigenetic changes could be identified, and quantification of the percentage of probes falling into each group during the time course is shown in Figure 3C.

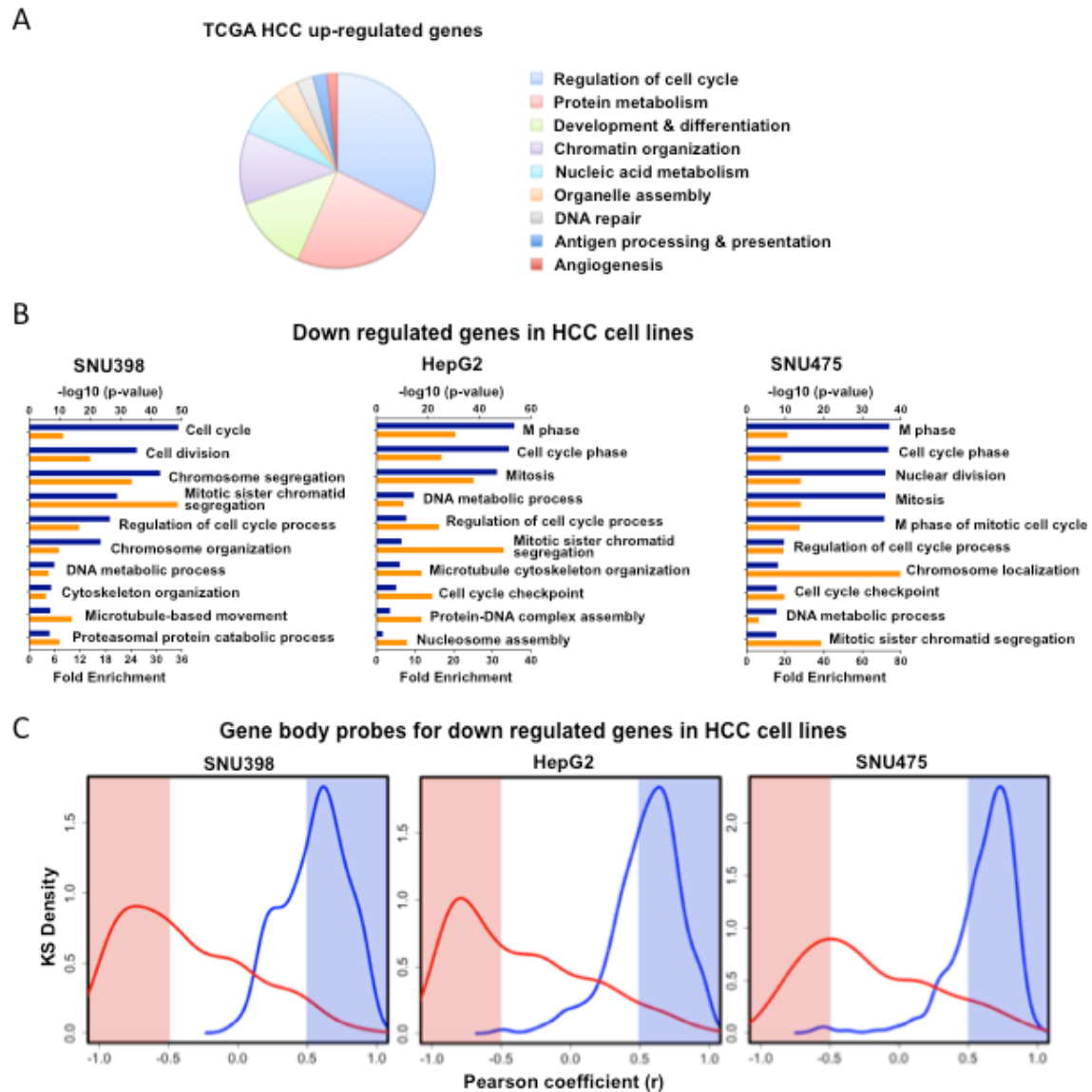


**Figure S6.** Related to Figure 5, analysis of the frequently up-regulated genes in TCGA HCC tumors. (A) Gene Ontology (GO) analysis of frequently up regulated genes from TCGA HCC tumors. Pie charts show clusters of GO Biological Process (BP) terms using DAVID Bioinformatics Resources 6.8 with enrichment score  $>1$  and  $p$ -value  $<0.05$ . (B) Bar graphs show top 10 GO BP terms of genes frequently up regulated in TCGA HCC tumors that are down regulated by SGI-110 treatment in SNU398, HepG2 and SNU475 cells. Blue bars represent  $-\log_{10}$  ( $p$ -value) and orange bars represent fold enrichment scores. (C) Kernel density plots for genes in B show the Pearson correlation ( $r$ ) between gene expression and DNA methylation (blue lines) or nucleosome accessibility (red lines). Blue

shades highlight the probes that exhibit a significant positive correlation ( $r > 0.5$ ) between DNA methylation and expression, while red shades highlight the probes with a significant negative correlation ( $r < -0.5$ ) between nucleosome accessibility and expression.

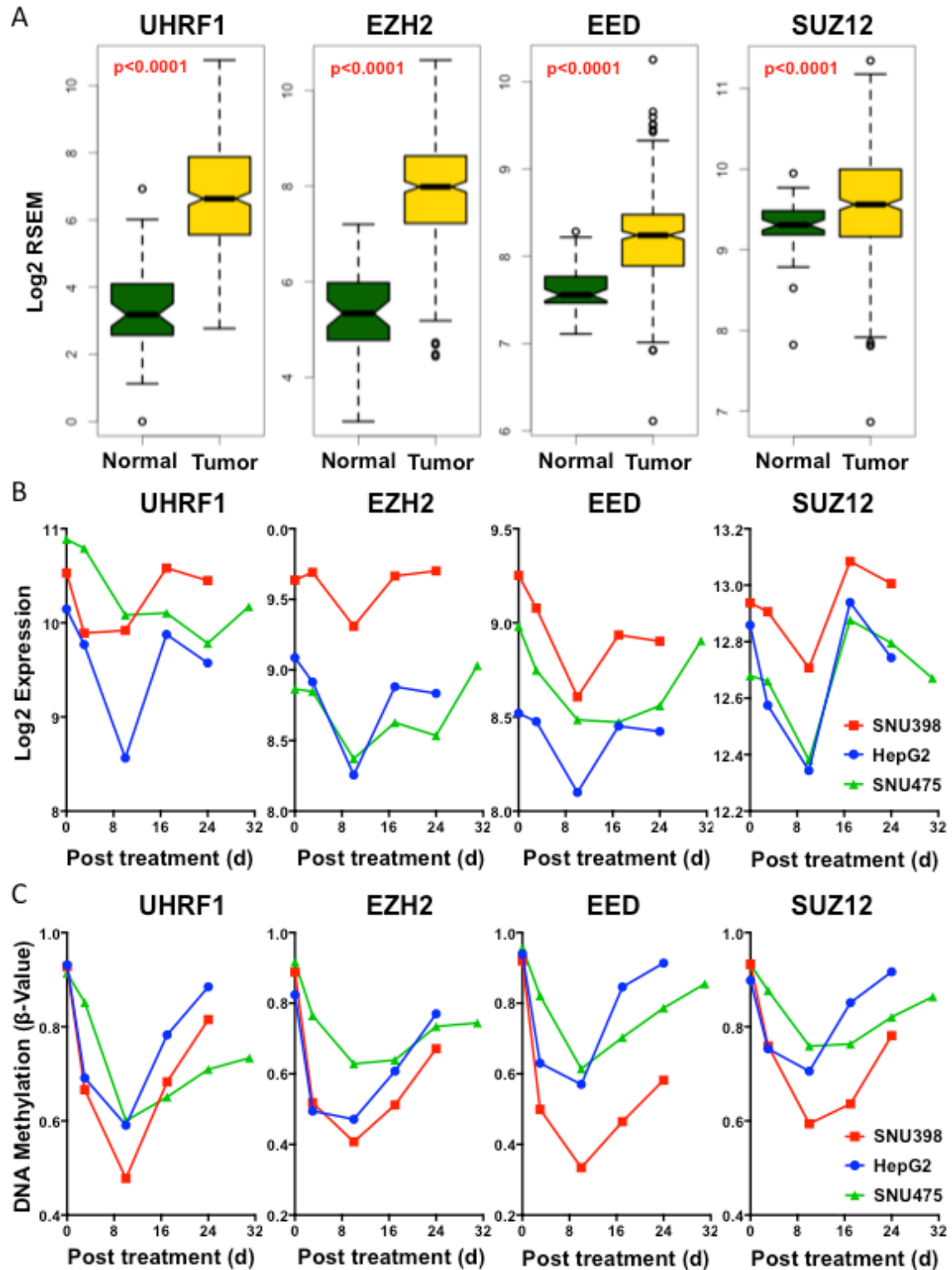


**Figure S7.** Epigenetic regulators *UHRF1*, *EZH2*, *EED* and *SUZ12* are overexpressed in primary HCC tumors and are down regulated by SGI-110

treatment. (A) Box plots show up regulation of *UHRF1*, *EZH2*, *EED* and *SUZ12* in primary TCGA HCC tumors compared to normal liver tissues. Normalized read counts were calculated for 50 normal (green box) and 374 tumor tissue (yellow box) samples using RNA-seq by Expectation-Maximization (RSEM). Wilcoxon rank-sum test was used to assess statistical significance. (B and C) Expression (B) and gene body methylation (C) levels of *UHRF1*, *EZH2*, *EED* and *SUZ12* in a time course upon SGI-110 treatment in SNU398, HepG2 and SNU475 cells.

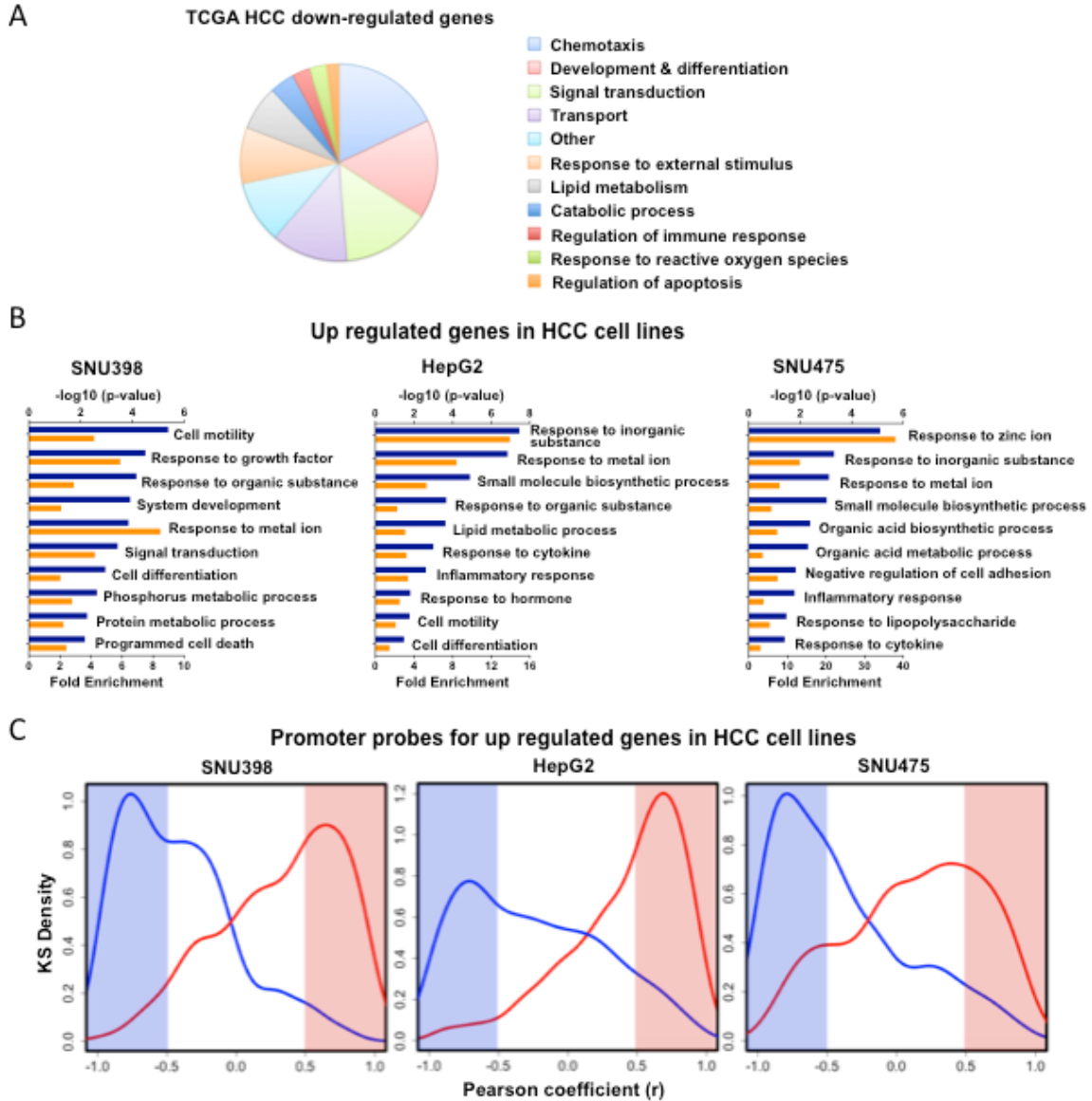


**Figure S8.** Related to Figure 6, analysis of the frequently down-regulated genes in TCGA HCC tumors. (A) Gene Ontology (GO) analysis of frequently down regulated genes from TCGA HCC tumors. Pie charts show clusters of GO Biological Process (BP) terms using DAVID Bioinformatics Resources 6.8 with enrichment score >1 and p-value <0.05. (B) Bar graphs show top 10 GO BP terms of genes frequently down regulated in TCGA HCC tumors that are up regulated by SGI-110 treatment in SNU398, HepG2 and SNU475 cells. Blue bars represent  $-\log_{10}(\text{p-value})$  and orange bars represent fold enrichment scores. (C) Kernel density plots for genes in B show the Pearson correlation ( $r$ ) between

gene expression and DNA methylation (blue lines) or nucleosome accessibility (red lines). Blue shades highlight the probes that exhibit a significant negative correlation ( $r < -0.5$ ) between DNA methylation and expression, while red shades highlight the probes with a significant positive correlation ( $r > 0.5$ ) between nucleosome accessibility and expression.

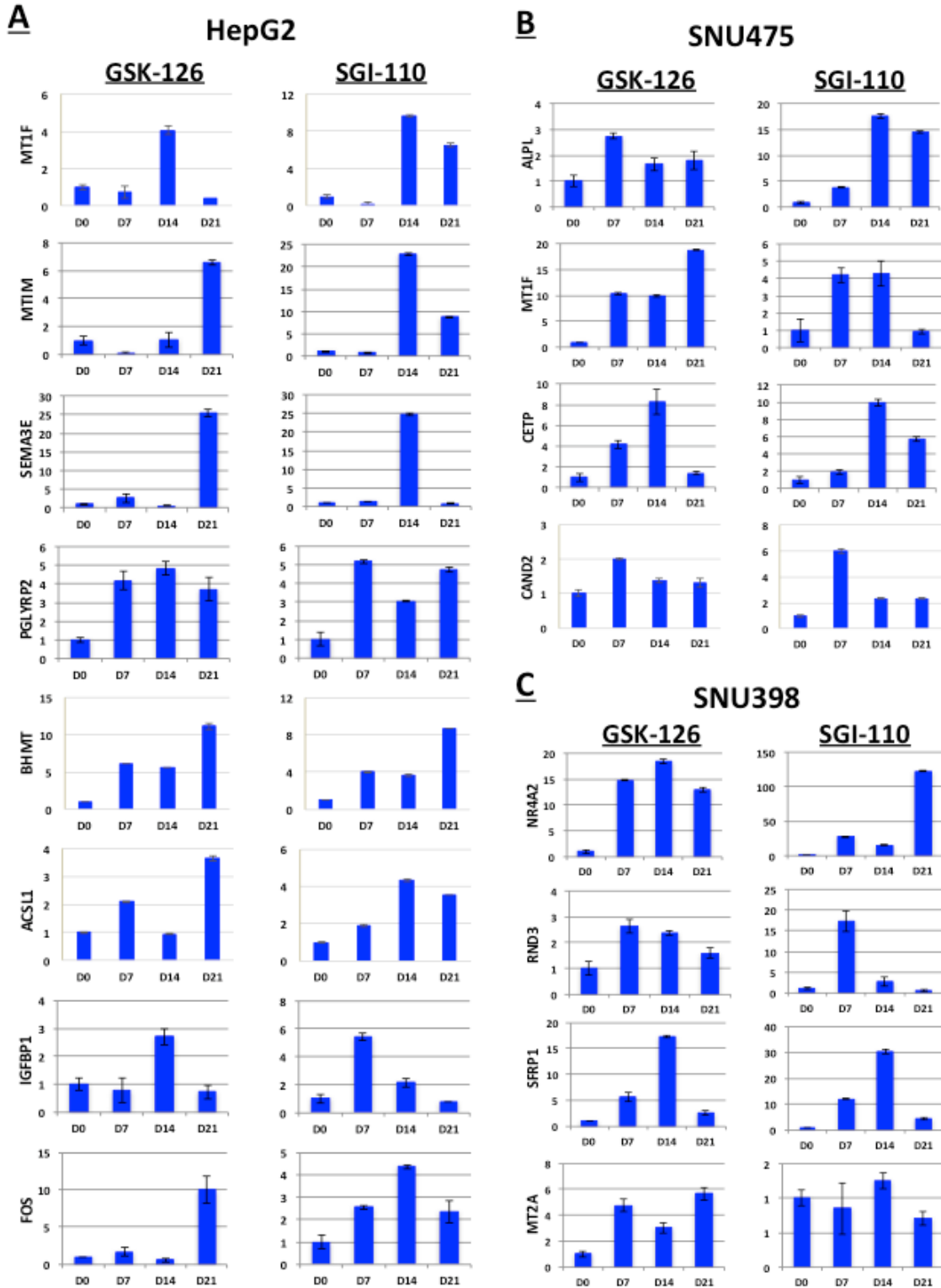


**Figure S9.** Up-regulation of SGI-110 target genes after EZH2i GSK-126 treatment in HepG2, SNU398 and SNU475 cells. Cells were treated with daily



doses of GSK-126 at 500 nM, or three daily consecutive doses of SGI-110 at 100 nM. At 0, 7, 14 and 21 days after the treatment, cells were harvested and gene expression was measured using quantitative RT-PCR. The expression of all genes was normalized to glyceraldehyde 3-phosphate dehydrogenase (GAPDH), and is presented as fold change to the expression values at Day 0 from four independent experiments.